Planetary and Space Science ∎ (∎∎∎∎) ∎∎∎–∎∎∎

Contents lists available at ScienceDirect

Planetary and Space Science

journal homepage: www.elsevier.com/locate/pss

Calibrating Mars Orbiter Laser Altimeter pulse widths at Mars Science Laboratory candidate landing sites

Wil Poole [a,b,*], Jan-Peter Muller [a,b], Sanjeev Gupta [c], Peter M. Grindrod [d,b]

[a] Imaging Group, The Mullard Space Science Laboratory, University College London, Holmbury St. Mary, Dorking RH5 6NT, UK
[b] Centre for Planetary Sciences, University College London, Gower Street, London WC1E 6BT, UK
[c] Department of Earth Science & Engineering, Imperial College London, South Kensington Campus, London SW7 2AZ, UK
[d] Department of Earth and Planetary Sciences, Birkbeck, University of London, Malet Street, London WC1E 7HX, UK

ARTICLE INFO

Article history:
Received 6 February 2014
Received in revised form
12 May 2014
Accepted 15 May 2014

Keywords:
Mars
MOLA
MSL
Surface roughness

ABSTRACT

Accurate estimates of surface roughness allow quantitative comparisons between planetary terrains. These comparisons enable us to improve our understanding of commonly occurring surface processes, and develop a more complete analysis of candidate landing and roving sites. A (secondary) science goal of the Mars Orbiter Laser Altimeter was to map surface roughness within the laser footprint using the backscatter pulse-widths of individual pulses at finer scales than can be derived from the elevation profiles. On arrival at the surface, these pulses are thought to have diverged to between 70 and 170 m, corresponding to surface roughness estimates at 35 and 70 m baselines respectively; however, the true baseline and relationship remains unknown. This work compares the Mars Orbiter Laser Altimeter pulse-widths to surface roughness estimates at various baselines from high-resolution digital terrain models at the final four candidate landing sites of Mars Science Laboratory. The objective was to determine the true baseline at which surface roughness can be estimated, and the relationship between the surface roughness and the pulse-widths, to improve the reliability of current global surface roughness estimates from pulse-width maps. The results seem to indicate that pulse-widths from individual shots are an unreliable indicator of surface roughness, and instead, the pulse-widths should be downsampled to indicate regional roughness, with the Slope-Corrected pulse-width dataset performing best. Where Rough Patches are spatially large compared to the footprint of the pulse, pulse-widths can be used as an indicator of surface roughness at baselines of 150–300 m; where these patches are spatially small, as observed at Mawrth Vallis, pulse-widths show no correlation to surface roughness. This suggests that a more complex relationship exists, with varying correlations observed, which appear to be dependent on the distribution of roughness across the sites.

1. Introduction

Accurate estimates of surface roughness allow for quantitative comparisons of surface descriptions leading to improved understanding of formation processes, improved identification of landing site hazards and calibration of radar returns, and more accurate estimates of aerodynamic roughness used in terrain–atmosphere interactions within climate modelling (Heavens et al., 2008; Holt et al., 2008; Kreslavsky and Head, 1999, 2000; Plaut and Garneau, 1999; Shepard et al., 2001). This makes it a useful tool for studying Mars, where quantitative characterisation of terrain can help us unlock the history of surface evolution after drawing comparisons with Earth analogues. Using estimates of aerodynamic roughness, such as that in Marticorena et al. (2006), we can further our understanding of the surface conditions under which dust lifting occurs, which can lead to the formation of global dust storms that can grow from local storms within weeks, obscuring almost the entire surface of the planet (Fenton et al., 2007; Listowski et al., 2011). Our aim is to study how the pulse-width of laser altimeter backscatter shots from the surface of Mars can be used to estimate surface roughness globally at a smaller length-scales than can be derived from along-track topographic profiles alone (Neumann et al., 2003). Theoretically derived global surface roughness maps have been produced and used since this pulse-width data was first collected, however a literature search shows that the actual relationship between these pulse-widths and 'ground-truth' has yet to be found.

* Corresponding author at: Imaging Group, The Mullard Space Science Laboratory, University College London, Holmbury St. Mary, Dorking RH5 6NT, UK.
E-mail address: william.poole.10@ucl.ac.uk (W. Poole).

http://dx.doi.org/10.1016/j.pss.2014.05.012

To date, there is no commonly accepted scientific definition of planetary surface roughness, referred to simply as surface roughness, and as a result many definitions exist (Shepard et al., 2001; Kreslavsky and Head, 2000; Rosenburg et al., 2011; Kreslavsky et al., 2013). Here, it is defined *as a measure of the vertical exaggerations across a horizontal plane or profile, at a defined baseline*. It is important to understand that surface roughness is variable, and as such changes depending upon the length scale at which it is measured. This length scale is known as the baseline, and can range from centimetres to kilometres. The common methods of measuring planetary surface roughness are outlined in Shepard et al. (2001), with the chosen method often dependent on the data type and the field. Kreslavsky et al. (2013) discuss the difficulties in choosing an intuitive, which allows a researcher to interpret and compare roughness, and stable measure of surface roughness, whereby anomalously high or low elevations or slopes across a plane or a profile can significantly affect the estimated surface roughness value for that plane or profile. The measure used here is the root-mean-square (RMS) height, as defined in Shepard et al. (2001), which can be considered as unstable (Kreslavsky et al., 2013). However, experience using ICESat pulse-widths over bare-earth terrains shows this method to perform best, compared to the interquartile range, which is considered to be more stable (Kreslavsky et al., 2013).

High-resolution images (0.25 m/pixel) and digital terrain models (DTMs) (1 m/pixel) from the High Resolution Imaging Science Experiment (HiRISE) provide unprecedented views of another planetary surface, albeit at the sacrifice of spatial coverage (McEwen et al., 2007, 2010). Therefore, surface roughness at fine-scales ($\lesssim 100$ m) cannot be derived globally. An alternative is to employ the Mars Orbiter Laser Altimeter (MOLA) to measure surface roughness from topographic profiles with ≈ 300 m along-track shot spacing and large (≈ 4 km at equator) inter-track spacing (Smith et al., 2001). The primary science objective of MOLA was to produce a global elevation model that would be useful for planetary scientists to quantify topographic variation on Mars, and to quantitatively characterise the Martian landscape and the processes governing its formation and evolution (Smith et al., 1999). A secondary science goal was to characterise the terrain at finer scales by recording the time-spread of the backscatter pulse, known as the pulse-width, from which surface characteristics from within the pulse-footprint can be derived (Smith et al., 2001). Part of the reflected pulse is collected by the receiver telescope and triggers one of the four receiver channels (Smith et al., 2001) (Fig. 1). Theoretically, the pulse-width of the received backscatter pulse, once corrected for instrumental and slope effects, can be used as an indicator of surface roughness within the footprint of the pulse, which was assumed to be 170 m (Smith et al., 2001). This was thought to correspond to surface roughness estimates at 100 m baselines, however the footprint size was revised in Neumann et al. (2003) to 75 m in the production of the Slope-Corrected pulse-width

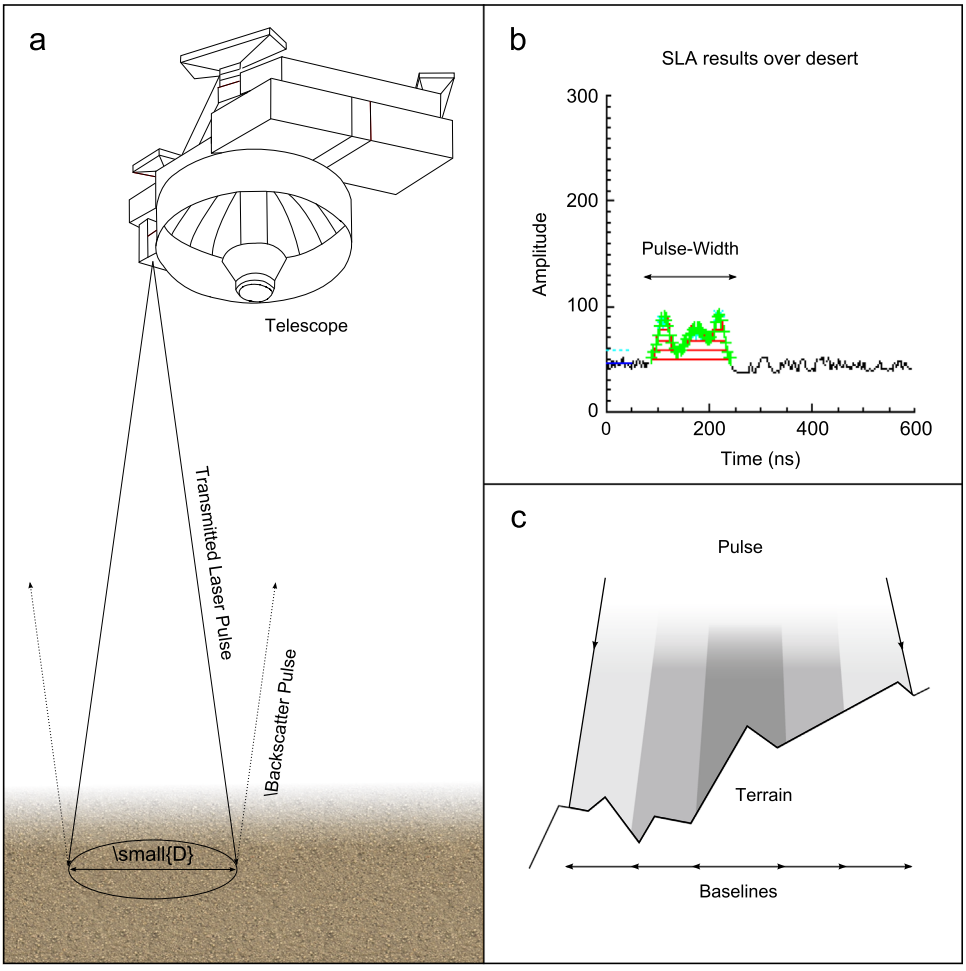

Fig. 1. (a) The MOLA instrument with an illustration of how a laser pulse diverges as it travels towards the surface of Mars before being reflected back towards the receiver telescope. (b) An example backscatter pulse over Earth desert terrain from the Shuttle Laser Altimeter (Garvin et al., 1998). Full pulse profiles are not available for Mars, instead only the final pulse-widths are available, shown by the time spread of the data plotted in the hashed region. (c) A schematic of how different pulse divergences can affect the size of roughness elements for which we have information. Smaller pulse divergence may tell us about large rocks, whereas larger divergences may tell us more about surface slope.

Please cite this article as: Poole, W., et al., Calibrating Mars Orbiter Laser Altimeter pulse widths at Mars Science Laboratory candidate landing sites. Planetary and Space Science (2014), http://dx.doi.org/10.1016/j.pss.2014.05.012

dataset, which is thought to indicate surface roughness at a baseline of approximately 35 m. Anderson et al. (2003) found that MOLA pulse-widths can be used to indicate surface properties at 100 m scale by comparing estimates from MOLA to ground truth data from the Mars Exploration Rovers. However, the pulse-width datasets have not been fully calibrated against surface roughness estimates from high-resolution terrain data, so the actual baseline at which the pulse-width datasets respond to surface roughness remains unknown (Neumann et al., 2003; Smith et al., 1999, 2001). Pulse-widths within the Precision Experimental Data Record (PEDR) version L dataset were corrected for only along-track slope in Smith et al. (2001) to produce estimates of vertical roughness. Neumann et al. (2003) identified and removed poor data from the PEDR dataset, which included cloud affected and saturated shots, as well as those taken at off-nadir angles greater than 1.5°. It was the early shots in the mission that were saturated, either digitally or electronically, and lead to under- or over-estimation of the pulse-width (Neumann et al., 2003; Smith et al., 2001). Neumann et al. (2003) also made additional across-track slope corrections to the pulse-width values using the 1 km MOLA gridded elevation dataset.

The work outlined here sets out to explore how MOLA pulse-widths compare to surface roughness estimates from high-resolution data to find the baseline, and best-fit relationship, at which they can reliably indicate roughness. In effect, this will calibrate the pulse-widths to 'ground-truth' data, which should produce a more reliable global map of *fine-scale* ($\leq$ 100 m) surface roughness than we have at present, and at finer scales than derived from elevation profiles alone (Kreslavsky and Head, 1999, 2000). The final four candidate landing sites for Mars Science Laboratory (MSL) are used in this study, as they have the most extensive high-resolution stereo-derived DTM coverage from the HiRISE camera (Golombek et al., 2012; McEwen et al., 2010). HiRISE was used extensively to assess the scientific and engineering pros and cons of each candidate landing site, whereas elsewhere on Mars HiRISE DTM coverage is very sparse, with less than 1% of the surface covered (Golombek et al., 2012; McEwen et al., 2010). The 1 m/pixel DTMs (http://hirise.lpl.arizona.edu/dtm/, last accessed: 12/19/2013) are used here as they can be used to estimate surface roughness at both the baseline estimates of 100 m (PEDR) and 35 m (Slope-Corrected) from the MOLA datasets used here. Fig. 1(c) shows a schematic diagram of how finding the correct pulse divergence and the baseline at which the MOLA datasets best respond is important, so that the size of the Rough Patches to which MOLA responds can be ascertained. An example backscatter pulse from the Shuttle Laser Altimeter over desert terrain is shown in Fig. 1(b). This example is from an Earth orbiting Flight Model Prototype of the final MOLA instrument flown on board the NASA Shuttle in 1992. Full pulse profiles were not recorded on MOLA, instead only the final time-spread of the backscatter pulses are recorded, so a full echo profile analysis of the data is not possible.

2. Methods

HiRISE, High Resolution Stereo Camera (HRSC) and MOLA elevation data were downloaded from the Planetary Data System (PDS) collated into site specific Geographic Information System (GIS) projects. Orthorectified images and DTMs were provided from HiRISE and HRSC; for MOLA, PEDR elevation profiles and gridded data (1 km) were used. HiRISE data were downloaded from the online repository at the University of Arizona (http://hirise.lpl.arizona.edu), HRSC data were downloaded from NASAs Planetary Data System (PDS) (pds.nasa.gov), and MOLA data extracted from the MOLA PEDR (version L) (available from http://pds-geosciences.wustl.edu/missions/mgs/pedr.html) and gridded dataset available as part of the Integrated Software for Imagers and Spectrometers (ISIS) 3 core data download. Data coregistration was completed using a "hierarchical coregistration technique", as described in Kim and Muller (2009), with the lowest resolution data, the MOLA elevation data, used as a basemap. This assumes that the MOLA dataset is correctly georeferenced. HRSC DTM elevation values were then compared to the MOLA PEDR and gridded data elevation values to ensure both vertical and horizontal accuracy of the HRSC datasets, with work by Gwinner et al. (2009, 2010) suggesting that HRSC DTMs are co-registered to MOLA with a Root-Mean-Square-Error (RMSE) of 25 m.

Finally, the HiRISE orthorectified image and DTM data were coregistered by comparing the HRSC nadir image data (12.5 m/pixel) to the orthorectified images from HiRISE (0.25 m/pixel). The HiRISE DTMs (1 m/pixel) were then coregistered to the correctly georeferenced HiRISE orthorectified images, and the HiRISE DTM values were compared to those from the HRSC DTM (50 m/pixel) elevation values. Correct co-registration of the HiRISE datasets is vital if the correct surface roughness values are to be extracted at MOLA pulse locations. The HiRISE DTMs were mosaicked into one dataset for each site, using a mean elevation where DTMs overlap, unless the elevations differed significantly, in which the overlap regions were ignored.

The DTMs were checked for quality by producing slope maps (at 1 m baseline) from the mosaicked data. Doing so highlights mosaicking errors, as well as errors from the DTM production process, such as pits, spikes, patchwork effects, and linear features which are not present in the imagery. Small mosaicking errors were observed in regions and masked out of the study, however, these errors did not occur near MOLA data and so would not have affected the study and were too small to be clearly mapped in Fig. 2.

Surface roughness maps were produced at different baselines for each location ranging from 10 to 600 m, which were chosen to cover baselines much smaller and larger than the theoretical estimates of surface roughness baselines (Smith et al., 2001; Neumann et al., 2003). Surface roughness was calculated for all pixels using all the elevation values within a circular window, which had a diameter equal to the baseline at which surface roughness was to be measured. Surface roughness is measured using the root-mean-square (RMS) height, defined in Shepard et al. (2001) as

$$\xi = \left[\frac{1}{n-1}\sum_{i=1}^{n}(z(x_i)-\bar{z})^2\right]^{1/2}, \quad (1)$$

where n is the number of points sampled, $z(x_i)$ is the elevation at point x_i, and $\bar{z}$ is the mean z for all the sample points within the window. The DTM data was not detrended before surface roughness was calculated, as the pulse-widths had been corrected for along-track slopes on the order of 600 m, or bidirectional slopes from the 1 km gridded MOLA dataset, significantly larger than the theoretical footprint scale slopes (35–100 m) (Neumann et al., 2003; Smith et al., 1999, 2001).

Data from both the PEDR and the Slope-Corrected datasets were then extracted within a region of interest for each site, and mapped with the other datasets and the surface roughness maps. From the PEDR, the received optical pulse-width was used as the pulse-width value, which has been corrected for filter characteristics and threshold settings to give an estimate of the roughness of the surface within the footprint of the pulse. A further investigation, using this dataset, was conducted using the shots that triggered receiver channel 1, considered to be the most reliable dataset, and known here as the Trigger 1 dataset (Smith et al., 1999). Surface roughness values were then extracted from each map at the centre of each MOLA pulse location, as given in each of the pulse-width datasets. These pulse-width values were then plotted against the extracted surface roughness values for each baseline separately. The R-squared values of a linear line-of-best-fit were calculated with pulse-width on RMS height, and the

Please cite this article as: Poole, W., et al., Calibrating Mars Orbiter Laser Altimeter pulse widths at Mars Science Laboratory candidate landing sites. Planetary and Space Science (2014), http://dx.doi.org/10.1016/j.pss.2014.05.012

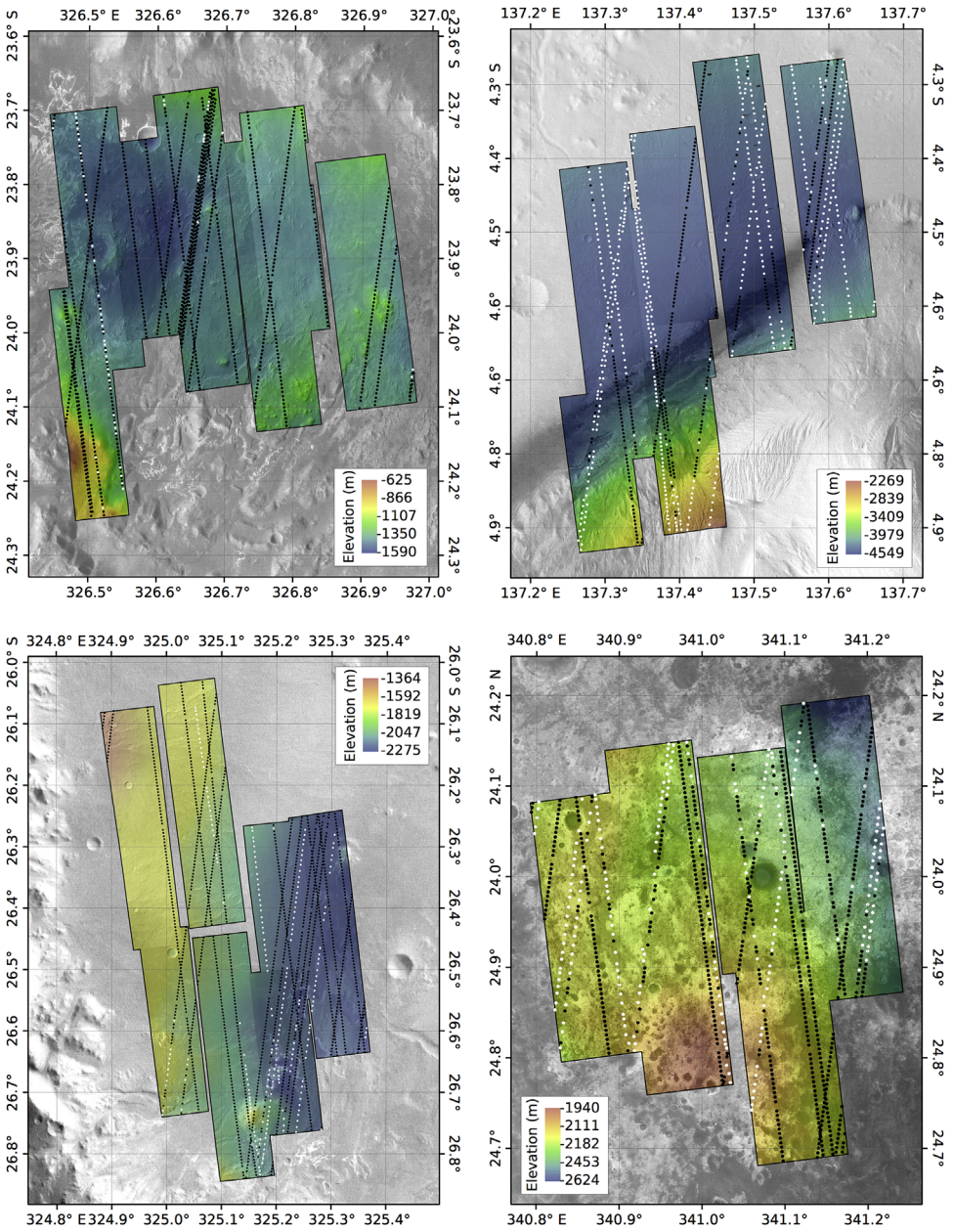

Fig. 2. Maps of each site with HiRISE image and DTM data shown in colour, with MOLA pulse locations superimposed and HRSC image in background. Black spots show Slope-Corrected pulse-width data locations, whilst black and white together show the PEDR pulse locations. From top left to bottom right, Eberswalde Crater, Gale Crater, Holden Crater, and Mawrth Vallis. Slope-Corrected pulse locations are shown in black and PEDR locations are shown in black and white. Image Credit: NASA/JPL/University of Arizona/USGS (HiRISE Image and DTMs) and ESA/DLR/FU Berlin (HRSC). (For interpretation of the references to colour in this figure caption, the reader is referred to the web version of this paper.)

best correlating baseline was found by selecting the plot with the highest *R*-squared value. This was carried out for each pulse-width dataset, surface roughness method, and region separately.

3. Laser Altimeter pulse-width theory

The width of a received backscatter pulse, σ_r, which is theoretically derived in Gardner (1982), is given as

$$\sigma_r^2 = \sigma_t^2 + \sigma_l^2 + \sigma_f^2 + \sigma_b^2, \tag{2}$$

where σ_t are the effects due to terrain, σ_l is the width of the outgoing pulse (3.5 ns), and σ_f is the response of the instrument (8.5 ns on channel 1), and σ_b is the effect due to beam divergence, which is negligible (Neumann et al., 2003).

The terrain effects can be further expanded, as in Neumann et al. (2003), to estimate the effects of slope and deviations from this slope:

$$\sigma_t^2 = \sigma_m^2 + \frac{4R_m^2}{c^2}[\tan^2(\gamma)\ \tan^2(\theta)], \tag{3}$$

where σ_m is due to the deviation from the slope within the footprint, R_m is the one-way laser range, c is the speed of light, γ is the RMS divergence angle, and θ is the surface slope.

No further corrections are made to the pulse-widths within the datasets in this work, which compares the pulse-widths derived within the three datasets outlined in Section 2 to surface

Please cite this article as: Poole, W., et al., Calibrating Mars Orbiter Laser Altimeter pulse widths at Mars Science Laboratory candidate landing sites. Planetary and Space Science (2014), http://dx.doi.org/10.1016/j.pss.2014.05.012

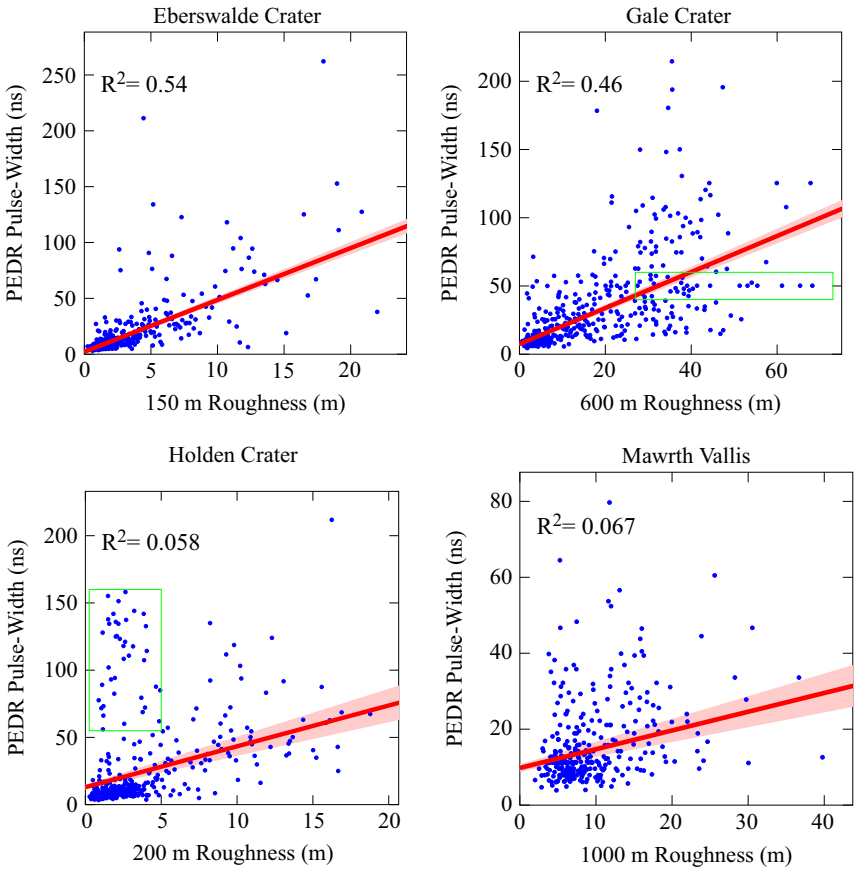

Fig. 3. The best correlated plots of the tested baselines using the PEDR pulse-widths for each of the study sites. The *R*-squared values are shown in the top-left of each plot, and the best correlation baseline is shown in the *y*-axis label. The boxes show regions of poor data within the PEDR pulse-width data that were excluded in the Neumann et al. (2003) dataset.

roughness derived from the HiRISE DTMs. Thus we are effectively comparing σ_t to the height variability within the footprint of the pulse, albeit with the Slope-Corrected dataset removing the effect of long baseline slopes. For this reason, the DTM data is not detrended to remove the effect of background slope.

4. Results

Plots showing the best correlated plots from each region using the PEDR, Trigger 1, and Slope-Corrected pulse-widths plotted against the RMS height are shown in Figs. 3, 4, and 5 respectively. All the results discussed here are significant at the 95% confidence level.

Of all the sites, Eberswalde Crater consistently showed the highest *R*-squared values for each of the three pulse-width datasets. The Slope-Corrected pulse-width dataset revealed the highest *R*-squared values, as expected. The slope of the line-of-best-fit for the Slope-Corrected pulse-widths is similar to those observed when the PEDR pulse-widths are used. For Eberswalde Crater, the *R*-squared values were not improved when using the Trigger 1 pulse-widths, compared to the other pulse-width datasets, as shown in Table 1. The highest *R*-squared value of 0.6 using the Slope-Corrected pulse-widths suggests that MOLA pulse-widths may not be reliable enough to be used in the selection of landing and roving sites.

Gale Crater reveals the next highest *R*-squared values, when averaged across the three pulse-width datasets. Here, the highest correlations occur at larger baselines than typically observed at Eberswalde Crater, with the highest *R*-squared value occurrence using the PEDR pulse-widths. It is, however, clear that this dataset contains many erroneous data points, which have been removed in the Slope-Corrected dataset. This is particularly evident in Fig. 3, which shows a string of erroneous points occurring at 51 ns at varying surface roughness values, shown in the box in Fig. 3; these data occur in a single orbit. It happens that this string of poor data sits close to the line-of-best-fit in the PEDR pulse-width plot, and thus improves the *R*-squared value compared to the Slope-Corrected plot. Gale Crater has the most number of points removed, of the 1571 points present in the PEDR dataset, only 1271 and 433 points are present in the Trigger 1 and Slope-Corrected datasets respectively. The fact that less than a third of the PEDR data points remain in the Slope-Corrected dataset suggests that despite presenting the lower *R*-squared value, the Slope-Corrected dataset is the most reliable. The highest correlation baseline for the Slope-Corrected pulse-width plot is 300 m, twice that found at Eberswalde Crater.

Holden Crater presents the largest change in *R*-squared values when comparing across the three MOLA pulse-width datasets. A very low *R*-squared value was found in the PEDR pulse-width plot despite there appearing to be a clear relationship of points around the line-of-best-fit in Fig. 3. This result is caused by a group of poor quality data that exists between pulse-widths of 50–150 ns, and 0–5 m surface roughness values. These data are not present in the Trigger 1 or Slope-Corrected pulse-width datasets, and as a result the *R*-squared value is significantly improved. This finding suggests that the identification of poor data is very important in improving the correlation between surface roughness and MOLA pulse-widths. The slope of the best-fit line is similar to that found at Eberswalde Crater, which shows

Please cite this article as: Poole, W., et al., Calibrating Mars Orbiter Laser Altimeter pulse widths at Mars Science Laboratory candidate landing sites. Planetary and Space Science (2014), http://dx.doi.org/10.1016/j.pss.2014.05.012

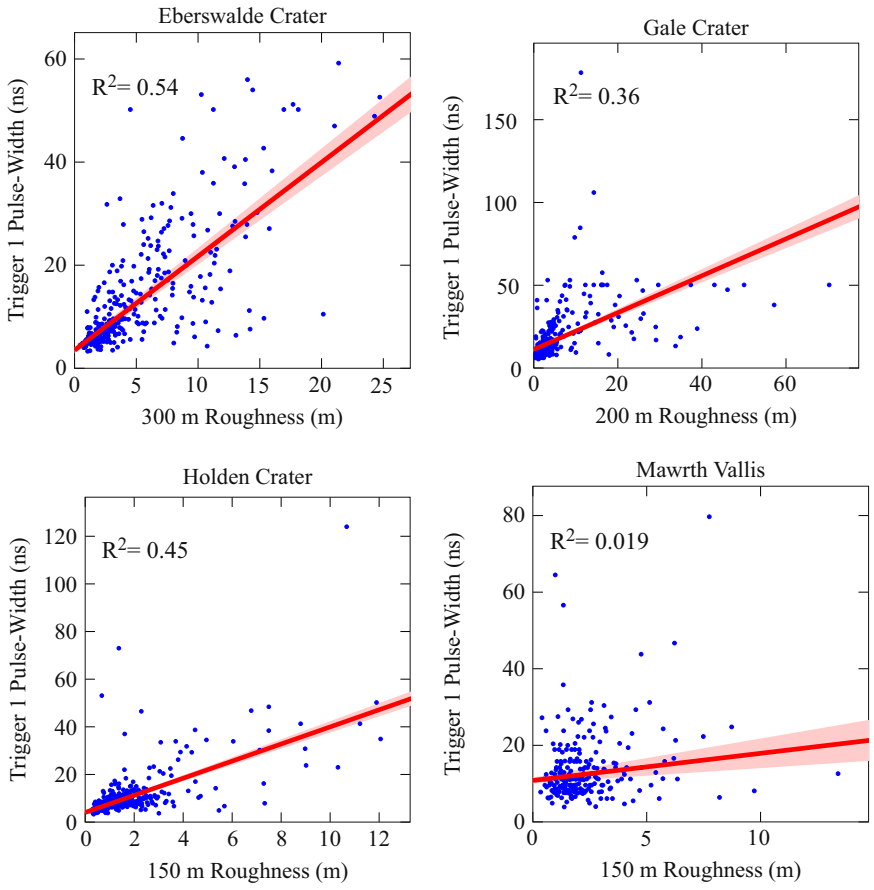

Fig. 4. The best correlated plots of the tested baselines using the Trigger 1 pulse-widths for each of the study sites. The *R*-squared values are shown in the top-left of each plot, and the best correlation baseline is shown in the *y*-axis label.

consistency within the dataset; these sites also reflect similar geological formation processes: impact craters which have then potentially been modified within a fluvial–lacustrine environment. The line-of-best-fit for the results from Gale Crater cannot be directly compared due to the different best correlation baselines.

At Mawrth Vallis, all pulse-width datasets showed very low *R*-squared values. As the *R*-squared values are so low the baselines, at which the best correlations occur, should be ignored. To explore why these low *R*-squared values only occur here, histograms of surface roughness and pulse-width distributions are shown in Fig. 6.

The distribution of surface roughness at 150 m (Fig. 6) is split into two distinct distributions: Eberswalde Crater and Gale Crater have similar distributions, as do Holden Crater and Mawrth Vallis. Holden Crater and Mawrth Vallis have similar distributions of surface roughness, which suggests that it is not the distribution of surface roughness which is the cause of the poor results observed at Mawrth Vallis. However, these sites do not share the same distribution of pulse-widths. Eberswalde Crater and Gale Crater show similar distributions for both surface roughness and pulse-widths. The distribution for Holden Crater decreases quickly after the peak, but has a long tail, which is expected given the lower frequency of very rough terrain shown in the surface roughness distribution. The distribution of pulse-widths at Mawrth Vallis, on the other hand, initially drops off slowly, but has a shorter tail, suggesting that very less rough terrain is detected. This result suggests that it is the detection of rough features, rather than the distribution of surface roughness, which causes the low *R*-squared value. To explore this finding further, maps of surface roughness and very rough terrain are shown in Fig. 7.

Fig. 7 shows only the spatial coverage of rough terrain, known as Rough Patches, considered here to have surface roughness values larger than 4 m at 150 m baselines. The 150 m baseline was chosen as it was the most commonly occurring baseline for two of the three sites which showed some correlation between surface roughness and MOLA pulse-widths, and it allows for direct comparisons between the spatial distribution and the extent of Rough Patches. A surface roughness value of 4 m was chosen as the threshold after reviewing the surface roughness distribution in Fig. 6, as the approximate point where all regions begin their long-tailed distributions. A visual inspection of the Rough Patches shows Eberswalde Crater and Gale Crater to have spatially large Rough Patches, which cover a significant proportion of the terrain. Here, large outcrops of rough terrain are interspersed with smoother terrain, which itself has some small outcrops of rough terrain associated with small impact craters and channel morphology; at Holden Crater the Rough Patches appear to be smaller, but follow a similar pattern. Mawrth Vallis shows a distinctly different pattern, whereby the typical Rough Patches typically appear to be much smaller. Larger patches of Rough Terrain are inhomogeneous and contain regions of smoother terrain within their boundary,to produce a spotty effect. Craters present in this terrain appear to be similar to those observed elsewhere, but are associated with some of the roughest features, unlike the other sites where channel morphology and extensive slopes appear to be roughest.

5. Discussion

For the first time, we have employed Geographical Information System (GIS) technology to do a detailed inter-comparison

Please cite this article as: Poole, W., et al., Calibrating Mars Orbiter Laser Altimeter pulse widths at Mars Science Laboratory candidate landing sites. Planetary and Space Science (2014), http://dx.doi.org/10.1016/j.pss.2014.05.012

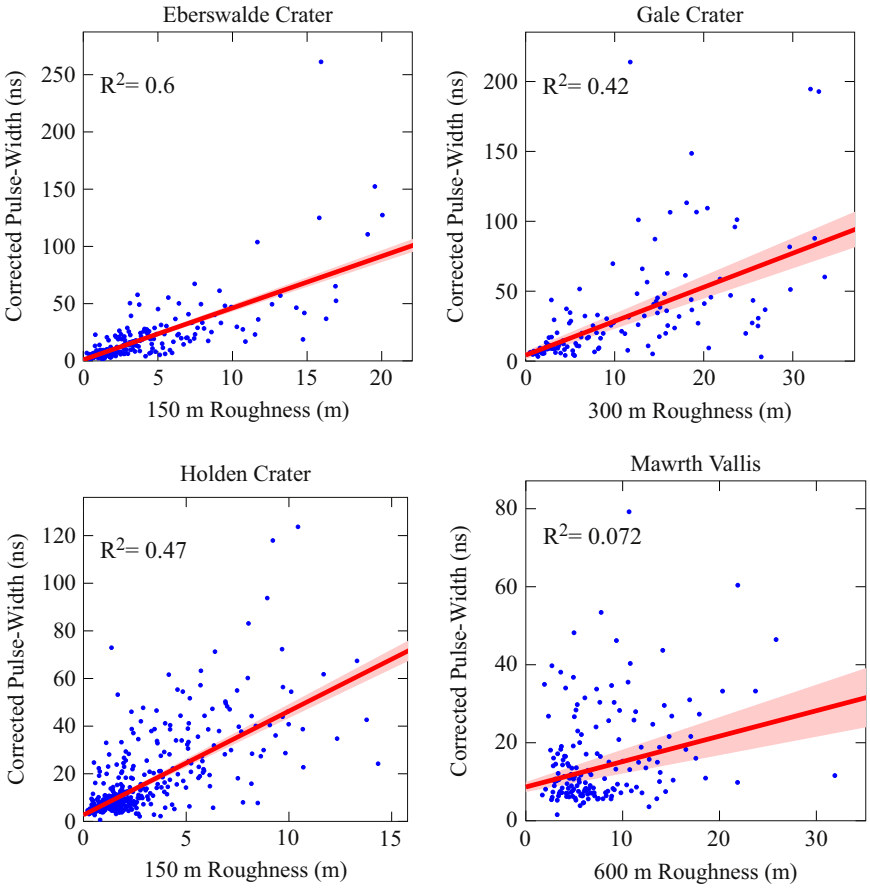

Fig. 5. The best correlated plots of the tested baselines using the Slope-Corrected pulse-widths for each of the study sites. The *R*-squared values are shown in the top-left of each plot, and the best correlation baseline is shown in the *y*-axis label.

Table 1
Observed *R*-squared values and the baselines at which these values occur for each of the three pulse-width datasets over the four sites.

MOLA Dataset	Eberswalde	Gale	Holden	Mawrth
PEDR				
R^2	0.54	0.46	0.06	0.07
Baseline (m)	150	600	200	1000
Shots	1410	1569	2031	1185
Trigger 1				
R^2	0.54	0.36	0.46	0.02
Baseline (m)	300	200	150	150
Shots	932	1271	1543	993
Slope-Corrected				
R^2	0.60	0.42	0.47	0.07
Baseline (m)	150	300	150	600
Shots	1157	433	1509	649

between spaceborne Laser Altimeter pulse-width data and high-resolution DTM data. The results suggest that the Slope-Corrected pulse-width dataset from Neumann et al. (2003) provides the best estimates of surface roughness, where surface roughness is measured using the RMS height. This dataset produced the highest observed *R*-squared values over Eberswalde Crater and Holden Crater, whereas at Gale crater the highest value is observed using the PEDR pulse-width dataset. Pulse-widths over Mawrth Vallis showed very low *R*-squared values for all pulse-width datasets and surface roughness baselines.

The removal of known poor data from the PEDR dataset in the production of the Slope-Corrected pulse-width dataset is the likely cause of the improved *R*-squared values over Eberswalde Crater and Holden Crater, where it is most pronounced at Holden Crater. Here, there is a significant collection of poor data at low surface roughness values and high pulse-widths using the PEDR pulse-width dataset, which are not present in the Trigger 1 and Slope-Corrected datasets. These poor data could be results from early in the mission, whereby the received shots saturated the receiver (Neumann et al., 2003; Smith et al., 2001). As a result, the *R*-squared values over this region using Trigger 1 and Slope-Corrected datasets are 0.46 and 0.47 respectively, compared to 0.06 using the PEDR data. The appearance of the Holden Crater Trigger 1 and Slope-Corrected pulse-width results also suggests that the generic removal of Triggers 2,3, and 4 data is not a reliable method of improving observed *R*-squared values, as doing so removes data at higher pulse-width and roughness values, which is considered to be good in the Slope-Corrected dataset. In addition, as the number of points in the Trigger 1 and Slope-Corrected pulse-width datasets is similar over Holden Crater, this shows that the same data are not being removed, hence poor data remains in the Trigger 1 dataset over this region.

At Gale Crater, the PEDR pulse-width dataset produces the highest *R*-squared values, which is attributed to a significant amount of poor data positioned close to the line-of-best-fit. Again, these poor data, especially those highlighted in the box in Fig. 3, could be attributed to saturated shots, hence not being present in the Slope-Corrected data (Neumann et al., 2003; Smith et al., 2001). The removal of this poor data in the Slope-Corrected dataset actually produces a lower *R*-squared value due to the lower density of data in and around the line-of-best-fit. Despite this, the Slope-Corrected dataset is considered to be the most

Please cite this article as: Poole, W., et al., Calibrating Mars Orbiter Laser Altimeter pulse widths at Mars Science Laboratory candidate landing sites. Planetary and Space Science (2014), http://dx.doi.org/10.1016/j.pss.2014.05.012

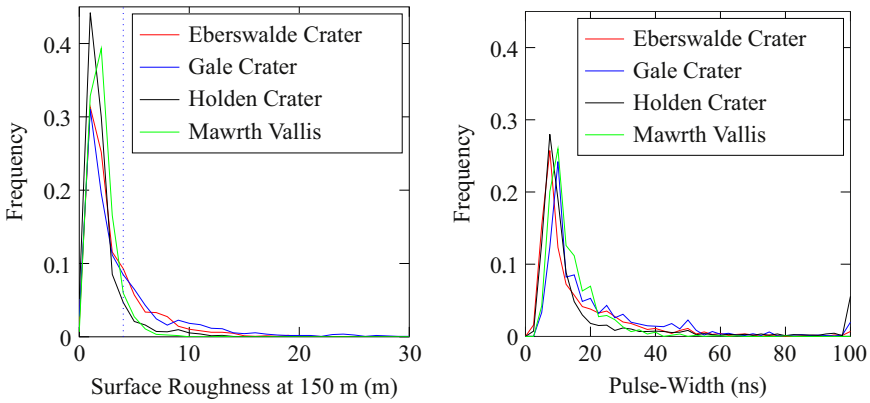

Fig. 6. Left: Surface roughness at 150 m baseline distribution for each site. Right: Pulse-width distribution at each site.

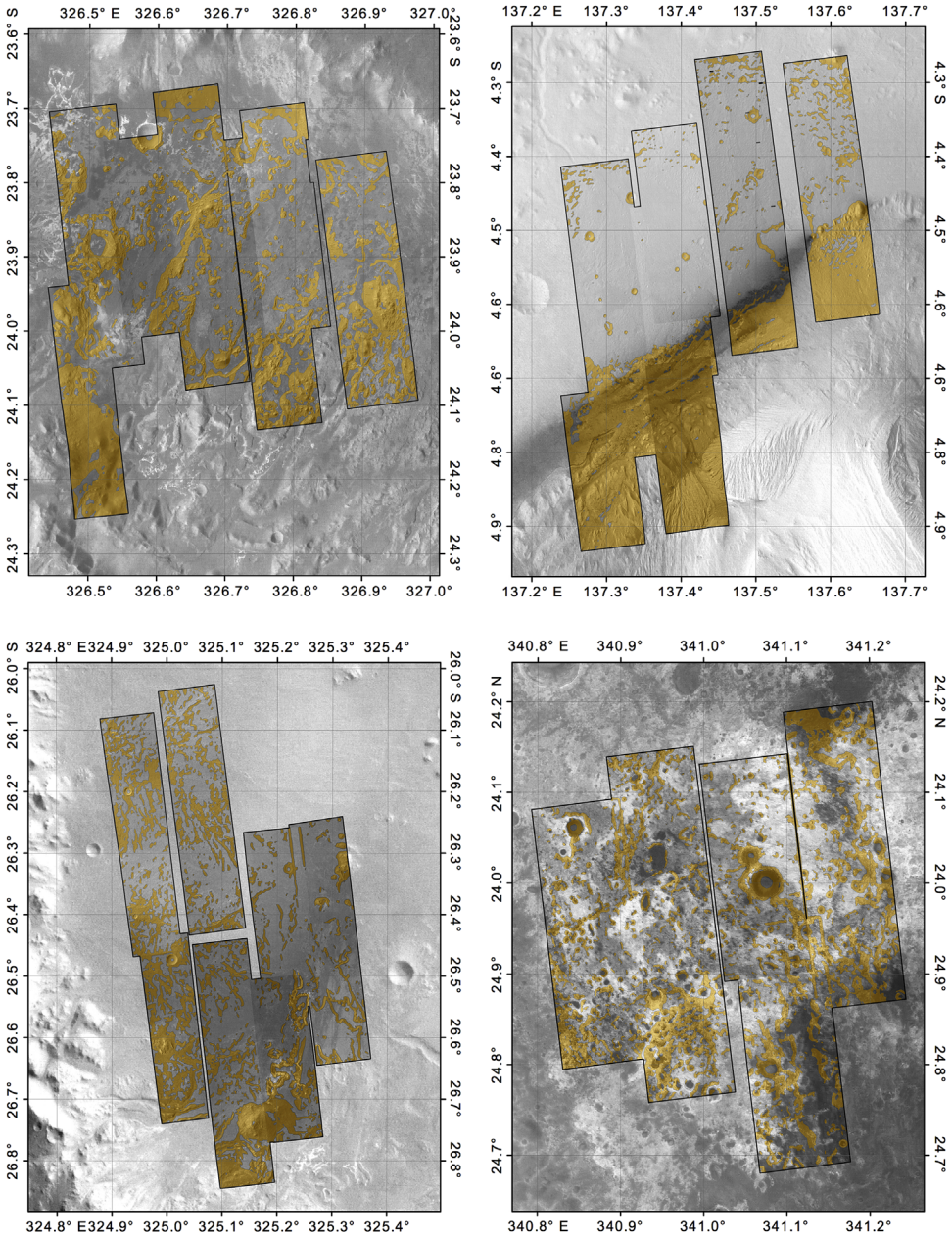

Fig. 7. Maps of areas considered rough (RMS height >4 m at 150 m baseline) for each site (orange). HiRISE images are shown within white boundary, with background HRSC image. From left to right: Eberswalde Crater and Gale Crater (both top), Holden Crater and Mawrth Vallis (both bottom). Image Credit: NASA/JPL/University of Arizona/USGS (HiRISE Image and DTMs) and ESA/DLR/FU Berlin (HRSC). (For interpretation of the references to colour in this figure caption, the reader is referred to the web version of this paper.)

Please cite this article as: Poole, W., et al., Calibrating Mars Orbiter Laser Altimeter pulse widths at Mars Science Laboratory candidate landing sites. Planetary and Space Science (2014), http://dx.doi.org/10.1016/j.pss.2014.05.012

reliable pulse-width source, as approximately 2/3 of the PEDR data over this region is considered to be poor by Neumann et al. (2003). Unlike over the Holden Crater site, using only the Trigger 1 data does not improve results; instead, many of the poor data points remain, shown by the large difference in the number of shots between the different datasets over this region in Table 1.

Using the Trigger 1 pulse-widths at Eberswalde Crater does not change the observed *R*-squared value compared to the PEDR pulse-widths, instead there is a change of baseline at which the best correlation occurs (Table 1). The fact that the number of shots using the Trigger 1 data over this region is smaller than the Slope-Corrected data shows that using this data only removes many shots considered to be of good quality in the Neumann et al. (2003) work. Again, the Slope-Corrected dataset is therefore assumed to be the most reliable of the three pulse-width datasets, as it removes data known to be poor, rather than the generic removal of many good data, as observed at Holden Crater, and has the highest observed *R*-squared value of the four sites.

So why do the results at Mawrth Vallis not follow similar patterns? The Mawrth Vallis plots in Figs. 3–5 show no correlation between MOLA pulse-widths and surface roughness, for each of the three pulse-width datasets used here. It is thought that the nature of Rough Patches within the terrain has an effect on the ability to discern roughness from the MOLA pulse-widths. At the previous three sites the extent of the Rough Patches appears to be large and continuous, therefore there is a higher probability for the MOLA footprints overlapping only rough or only smooth terrain than at Mawrth Vallis, where the smaller extent and the spotted appearance of the Rough Patches mean there is a higher probability that individual footprints will overlap both rough and smooth terrains. The nature of the echo pulses over Mawrth Vallis is therefore expected to be complex, which could lead to incorrect measurement of pulse-widths, given the on board calculated threshold for the pulse-width start and stop timing systems and the filtering system employed on MOLA, which matches the shots to one of the four channels: smooth, moderate, rough, and clouds (Smith et al., 2001). Overall, the instrument has poor overall sensitivity to surface roughness estimates from HiRISE DTMs where there is an observed correlation. This could be due to the low intensity of reflected light due to scattering of light in the atmosphere and from the surface across a pulse footprint as large as those observed here.

All this suggests that estimates of surface roughness from single shots cannot be used as an estimate of surface roughness. Instead, a downsampling of data to produce estimates of regional roughness using an average of shots should be used, as in Abshire et al. (2000) and Neumann et al. (2003). Furthermore, the sensitivity of the instrument may be limited to indicate whether a region is rough, moderate or smooth. Anderson et al. (2003) found their predictions of the MER landing sites to be true using MOLA pulse-width data, however these sites were smoother than those considered here due to the engineering constraints of the rovers.

As a common baseline has not been found here, it remains unknown whether the surface roughness is estimated at 150 or 300 m baselines. The pulse-width dataset considered to be most reliable here, the Slope-Corrected dataset from Neumann et al. (2003), produces the best correlations over the Eberswalde Crater and Holden Crater sites at the same 150 m baseline, but is this similarity due to the sites sharing similar morphology? By chance? Or are these examples of sites where the method "works"? This requires further investigation and as these terrains are not representative of the wide variety of terrains on Mars, the follow-up work explores MOLA pulse-widths over much rougher terrain. It is expected that a wider distribution of roughness could improve the observed *R*-squared values when MOLA pulse-widths are compared to surface roughness, and may help find a definitive baseline at which MOLA pulse-widths respond to surface roughness globally, rather than for individual terrains. Additionally, it improves the probability of the pulse-footprints overlapping only rough or only smooth terrain, removing the problem that could be causing the lack of observed correlation at Mawrth Vallis.

6. Conclusions

The principal conclusion to be drawn from this work is that individual MOLA pulse-width data cannot be used reliably to infer surface characteristics at pulse footprint scales for the selection of landing and roving sites. Instead, the work confirms that pulse-width data should be downsampled to give regional indications of roughness, by averaging over several shots, as observed in Abshire et al. (2000) and Neumann et al. (2003). The most reliable results were derived from the Slope-Corrected MOLA pulse-width dataset, primarily due to the removal of poor quality data, as well improved slope correction techniques applied to this dataset.

The observed correlations appear to be dependent on the nature of the rough terrain across the sites. Where the rough terrain is large in extent, there is a correlation between pulse-width and surface roughness, whereas where the rough terrain is spatially small and not uniform, there is no observed correlation. However, the work has been unable to find a common baseline at which the best correlations are observed, with best correlation baselines occurring at 150 to 300 m. With the highest *R*-squared value is 0.6, observed at Eberswalde Crater, there is a large scope for error even at sites where there appears to be a good correlation, and, as this is observed at 150 m baselines, this represents only a minor improvement in the understanding of global surface roughness compared to the along-track elevation profiles produced in Kreslavsky and Head (2000, 2002).

Ackowledgements

The authors would like to thank G. Neumann for providing us with the dataset produced in Neumann et al. [2003], and the reviewers for their suggestions in how to improve this paper. W. D.P. would like to thank STFC for his Ph.D. studentship (Grant ST/I506053/I), and P.M.G. would like to thank the UK Space Agency for funding (Aurora Fellowship Grants ST/J002127/1; ST/J005215/1).

References

Abshire, James B., Sun, Xiaoli, Afzal, Robert S., 2000. Mars Orbiter Laser Altimeter: receiver model and performance analysis. Appl. Opt. 39 (May (15)), 2449–2460, http://dx.doi.org/10.1364/AO.39.002449, URL ⟨http://www.opticsinfobase.org/ao/viewmedia.cfm?uri=ao-39-15-2449&seq=0⟩.

Anderson, F. Scott, Haldemann, Albert F.C., Bridges, Nathan T., Golombek, Matt P., Parker, Tim J., 2003. Analysis of MOLA data for the Mars exploration rover landing sites. J. Geophys. Res.: Planets 108 (December (E12)), http://dx.doi.org/10.1029/2003JE002125, URL ⟨http://onlinelibrary.wiley.com/doi/10.1029/2003JE002125/pdf⟩.

Fenton, Lori K., Geissler, Paul E., Haberle, Robert M., 2007. Global warming and climate forcing by recent albedo changes on Mars. Nature 446 (May), 646–649, http://dx.doi.org/10.1038/nature05718, URL ⟨http://www.nature.com/nature/journal/v446/n7136/pdf/nature05718.pdf⟩.

Gardner, C.S., 1982. Target signatures for laser altimeters: an analysis. Appl. Opt. 21 (February (3)), 448–453, http://dx.doi.org/10.1364/AO.21.000448, URL ⟨http://www.opticsinfobase.org/abstract.cfm?URI=ao-21-3-448⟩.

Garvin, James B., Bufton, J.L., Blair, J., Harding, David J., Luthcke, Scott B., Frawley, J.J., Rowlands, David D., 1998. Phys. Chem. Earth 23 (9–10), 1053–1068, http://dx.doi.org/10.1016/S0079-1946(98)00145-1, URL ⟨http://www.sciencedirect.com/science/article/pii/S0079194698001451/pdf?md5=29711a606fdcb2f8ac9080b799b18a56&pid=1-s2.0-S0079194698001451-main.pdf⟩.

Golombek, Matt P., Grant, J.A., Kipp, D.M., Vasavada, Ashwin R., Kirk, R.L., Fergason, R.L., Bellutta, P., Calef, F., Larsen, K., Katayama, Y., Huertas, A., Beyer, R.A., Chen, A., Parker, Tim J., Pollard, B., Lee, Steven W., Sun, Y., Hoover, R., Sladek, H., Grotzinger, John P., Welch, Richard V., Noe Dobrea, E.Z., Michalski, Joseph R., Watkins, M.M., 2012. Selection of the Mars science laboratory landing site.

Space Sci. Rev. 170 (September (1–4)), 641–737, http://dx.doi.org/10.1007/s11214-012-9916-y, URL ⟨http://link.springer.com/content/pdf/10.1007%2Fs11214-012-9916-y.pdf⟩.

Gwinner, K., Scholten, F., Spiegel, M., 2009. Derivation and validation of high-resolution digital terrain models from Mars express HRSC-data. Photogramm. Eng. Remote Sens. 75 (9), 1127–1142, URL ⟨http://www.asprs.org/a/publications/pers/2009journal/september/2009_sep_1127-1142.pdf⟩.

Gwinner, K., Scholten, F., Preusker, F., Elgner, S., Roatsch, T., Spiegel, M., Schmidt, R., Oberst, Jurgen, Jaumann, R., Heipke, C., 2010. Topography of Mars from global mapping by HRSC high-resolution digital terrain models and orthoimages: characteristics and performance. Earth Planet. Sci. Lett. 294 (June (3–4)), 506–519, http://dx.doi.org/10.1016/j.epsl.2009.11.007, URL ⟨http://www.sciencedirect.com/science/article/pii/S0012821X09006542/pdfft?md5=27897f46791eed21be70afbf7498c32f&pid=1-s2.0-S0012821X09006542-main.pdf⟩.

Heavens, N.G., Richardson, Mark I., Toigo, Anthony D., 2008. Two aerodynamic roughness maps derived from Mars Orbiter Laser Altimeter (MOLA) data and their effects on boundary layer properties in a Mars general circulation model (GCM). J. Geophys. Res.: Planets 113 (January), http://dx.doi.org/10.1029/2007JE002991, URL ⟨http://onlinelibrary.wiley.com/doi/10.1029/2007JE002991/pdf⟩.

Holt, J.W., Safaeinili, A., Plaut, Jeffrey J., Head III, James W., Phillips, Roger J., Seu, R., Kempf, S.D., Choudhary, P., Young, D.A., Putzig, N.E., Biccari, D., Gim, Y., 2008. Radar sounding evidence for buried glaciers in the southern mid-latitudes of Mars. Science 322 (November), 1235–1238, http://dx.doi.org/10.1126/science.1164246, URL ⟨http://www.sciencemag.org/content/322/5905/1235.full.pdf⟩.

Kim, Jung-Rack, Muller, Jan-Peter, 2009. Multi-resolution topographic data extraction from Martian stereo imagery. Planet. Space Sci. 57 (November (14–15)), 2095–2112, http://dx.doi.org/10.1016/j.pss.2009.09.024, URL ⟨http://www.sciencedirect.com/science/article/pii/S0032063309002888/pdfft?md5=e8792d6efc3cdff7c88797cdd8851fda&pid=1-s2.0-S0032063309002888-main.pdf⟩.

Kreslavsky, M.A., Head III, James W., 1999. Kilometer-scale slopes on Mars and their correlation with geologic units: initial results from Mars Orbiter Laser Altimeter (MOLA) data. J. Geophys. Res.: Planets 104 (September (E9)), 21911–21924, http://dx.doi.org/10.1029/1999JE001051, URL ⟨http://onlinelibrary.wiley.com/doi/10.1029/1999JE001051/pdf⟩.

Kreslavsky, M.A., Head III, James W., 2000. Kilometer-scale roughness of Mars: results from MOLA data analysis. J. Geophys. Res.: Planets 105 (November (E11)), 26695–26711, http://dx.doi.org/10.1029/2000JE001259, URL ⟨http://onlinelibrary.wiley.com/doi/10.1029/2000JE001259/pdf⟩.

Kreslavsky, M.A., Head III, James W., 2002. Mars: nature and evolution of young latitude-dependent water-ice-rich mantle. Geophys. Res. Lett. 29 (August (15)), http://dx.doi.org/10.1029/2002GL015392, URL ⟨http://onlinelibrary.wiley.com/doi/10.1029/2002GL015392/pdf⟩.

Kreslavsky, Mikhail A., Head, James W., Neumann, Gregory A., Rosenburg, Margaret A., Aharonson, Oded, Smith, David E., Zuber, Maria T., 2013. Lunar topographic roughness maps from Lunar Orbiter Laser Altimeter (LOLA) data: scale dependence and correlation with geologic features and units. Icarus 226 (1), 52–66, http://dx.doi.org/10.1016/j.icarus.2013.04.027, URL ⟨http://linkinghub.elsevier.com/retrieve/pii/S0019103513001929⟩.

Listowski, C., Hébrard, E., Maattanen, A., Montmessin, F., Forget, François, 2011. A complete aerodynamic roughness maps derived from rock abundance data: extrapolation to high latitudes. In: The Fourth Annual Mars Atmosphere: Modelling and Observation, January, pp. 151–154, URL ⟨http://www-mars.lmd.jussieu.fr/paris2011/abstracts/listowski2_paris2011.pdf⟩.

Marticorena, B., Kardous, M., Bergametti, G., Callot, Y., Chazette, Patrick, Khatteli, Houcine, Le Hegarat-Mascle, Sylvie, Maille, Michel, Rajot, Jean-Louis, Vidal-Madjar, Mehrez, Zribi, Mehrez, 2006. Surface and aerodynamic roughness in arid and semiarid areas and their relation to radar backscatter coefficient. J. Geophys. Res.: Earth Surf. 111 (September (F3)), http://dx.doi.org/10.1029/2006JF000462, URL ⟨http://onlinelibrary.wiley.com/doi/10.1029/2006JF000462/pdf⟩.

McEwen, Alfred S., Eliason, Eric M., Bergstrom, James W., Bridges, Nathan T., Hansen, Candice J., Delamere, W. Alan, Grant, John A., Gulick, Virginia C., Herkenhoff, Kenneth E., Keszthelyi, Laszlo P., Kirk, Randolph L., Mellon, Micheal T., Squyres, Steven W., Thomas, Nicolas, Weitz, Catherine M., 2007. Mars reconnaissance Orbiter's high resolution imaging science experiment (HiRISE). J. Geophys. Res.: Planets 112 (May (E5)), http://dx.doi.org/10.1029/2005JE002605, URL ⟨http://onlinelibrary.wiley.com/doi/10.1029/2005JE002605/pdf⟩.

McEwen, Alfred S., Banks, M.E., Baugh, N., Becker, K.J., Boyd, A., Bergstrom, James W., Beyer, R.A., Bortolini, E., Bridges, Nathan T., Byrne, Shane, Castalia, Bradford, Chuang, Frank C., Crumpler, Larry S., Daubar, Ingrid J., Davatzes, Alix K., et al., 2010. The high resolution imaging science experiment (HiRISE) during MRO's primary science phase (PSP). Icarus 205 (January (1)), 2–37, http://dx.doi.org/10.1016/j.icarus.2009.04.023, URL ⟨http://www.sciencedirect.com/science/article/pii/S0019103509001808/pdfft?md5=1d463532ae9b205ebf2262d617926632&pid=1-s2.0-S0019103509001808-main.pdf⟩.

Neumann, Gregory A., Abshire, James B., Aharonson, Oded, Garvin, James B., Sun, Xiaoli, Zuber, Maria T., 2003. Mars Orbiter Laser Altimeter pulse width measurements and footprint-scale roughness. Geophys. Res. Lett. 30 (June (11)), 1561, http://dx.doi.org/10.1029/2003GL017048, URL ⟨http://onlinelibrary.wiley.com/doi/10.1029/2003GL017048/pdf⟩.

Plaut, Jeffrey J., Garneau, S., 1999. MOLA-derived roughness data used to predict surface scattering for Mars subsurface radar sounding. In: The Fifth International Conference on Mars, July, URL ⟨http://www.csa.com/partners/viewrecord.php?requester=gs&collection=TRD&recid=A9938912AH⟩.

Rosenburg, M.A., Aharonson, Oded, HeadIII, James W., Kreslavsky, M.A., Mazarico, Erwan M., Neumann, Gregory A., Smith, David E., Torrence, Mark H., Zuber, Maria T., 2011. Global surface slopes and roughness of the Moon from the Lunar Orbiter Laser Altimeter. J. Geophys. Res.: Planets 116 (February (E2)), http://dx.doi.org/10.1029/2010JE003716, URL ⟨http://onlinelibrary.wiley.com/doi/10.1029/2010JE003716/pdf⟩.

Shepard, Michael K., Campbell, Bruce A., Bulmer, Mark H., Farr, Tom G., Gaddis, Lisa R., Plaut, Jeffrey J., 2001. The roughness of natural terrain: a planetary and remote sensing perspective. J. Geophys. Res.: Planets 106 (December (E12)), 32777–32795, http://dx.doi.org/10.1029/2000JE001429, URL ⟨http://onlinelibrary.wiley.com/doi/10.1029/2000JE001429/pdf⟩.

Smith, David E., Zuber, Maria T., Solomon, Sean C., Phillips, Roger J., Head III, James W., Garvin, James B., Banerdt, W. Bruce, Muhleman, Duane O., Patterngill, Gordon H., Neumann, Gregory A., Lemoine, Frank G., Abshire, James B., Aharonson, Oded, Brown, C. David, Hauck, Steven A., Ivanov, Anton B., McGovern, Patrick J., Zwally, H. Jay, Duxbury, Thomas C., 1999. The global topography of Mars and implications for surface evolution. Science 284 (May), 1495–1503, http://dx.doi.org/10.1126/science.284.5419.1495, URL ⟨http://www.sciencemag.org/content/284/5419/1495.full.pdf⟩.

Smith, David E., Zuber, Maria T., Frey, Herbert V., Garvin, James B., Head III, James W., Muhleman, D.O., Pettengill, G.H., Phillips, R.J., Solomon, S.C., Zwally, H. Jay, Banerdt, W. Bruce, Duxbury, Thomas C., Golombek, Matt P., Lemoine, Frank G., Neumann, Gregory A., Rowlands, David D., Aharonson, Oded, Ford, P.G., Ivanov, Anton B., Johnson, C.L., McGovern, P.J., Abshire, James B., Afzal, Robert S., Sun, Xiaoli, 2001. Mars Orbiter Laser Altimeter: experiment summary after the first year of global mapping of Mars. J. Geophys. Res.: Planets 106 (October (E10)), 23689–23722, http://dx.doi.org/10.1029/2000JE001364, URL ⟨http://onlinelibrary.wiley.com/doi/10.1029/2000JE001364/pdf⟩.

Please cite this article as: Poole, W., et al., Calibrating Mars Orbiter Laser Altimeter pulse widths at Mars Science Laboratory candidate landing sites. Planetary and Space Science (2014), http://dx.doi.org/10.1016/j.pss.2014.05.012